doi:10.1093/brain/aww347 BRAIN 2017: 140; 692–706 | 692

BRAIN
A JOURNAL OF NEUROLOGY

Synaptic inputs from stroke-injured brain to grafted human stem cell-derived neurons activated by sensory stimuli

Daniel Tornero,[1] Oleg Tsupykov,[2] Marcus Granmo,[3] Cristina Rodriguez,[1] Marita Grønning-Hansen,[1] Jonas Thelin,[3] Ekaterina Smozhanik,[2] Cecilia Laterza,[1] Somsak Wattananit,[1] Ruimin Ge,[1] Jemal Tatarishvili,[1] Shane Grealish,[4] Oliver Brüstle,[5] Galina Skibo,[2] Malin Parmar,[4] Jens Schouenborg,[3] Olle Lindvall[1] and Zaal Kokaia[1]

Transplanted neurons derived from stem cells have been proposed to improve function in animal models of human disease by various mechanisms such as neuronal replacement. However, whether the grafted neurons receive functional synaptic inputs from the recipient's brain and integrate into host neural circuitry is unknown. Here we studied the synaptic inputs from the host brain to grafted cortical neurons derived from human induced pluripotent stem cells after transplantation into stroke-injured rat cerebral cortex. Using the rabies virus-based trans-synaptic tracing method and immunoelectron microscopy, we demonstrate that the grafted neurons receive direct synaptic inputs from neurons in different host brain areas located in a pattern similar to that of neurons projecting to the corresponding endogenous cortical neurons in the intact brain. Electrophysiological *in vivo* recordings from the cortical implants show that physiological sensory stimuli, i.e. cutaneous stimulation of nose and paw, can activate or inhibit spontaneous activity in grafted neurons, indicating that at least some of the afferent inputs are functional. In agreement, we find using patch-clamp recordings that a portion of grafted neurons respond to photostimulation of virally transfected, channelrhodopsin-2-expressing thalamo-cortical axons in acute brain slices. The present study demonstrates, for the first time, that the host brain regulates the activity of grafted neurons, providing strong evidence that transplanted human induced pluripotent stem cell-derived cortical neurons can become incorporated into injured cortical circuitry. Our findings support the idea that these neurons could contribute to functional recovery in stroke and other conditions causing neuronal loss in cerebral cortex.

1 Laboratory of Stem Cells and Restorative Neurology, Lund Stem Cell Center, University Hospital, BMC B10, 221 84, Lund, Sweden
2 Bogomoletz Institute of Physiology, and State Institute of Genetic and Regenerative Medicine, 01024, Kyiv, Ukraine
3 Neuronano Research Center, Lund University, Scheelevägen 2, 223 81, Lund, Sweden
4 Developmental and Regenerative Neurobiology, Department of Experimental Medical Science, Wallenberg Neuroscience Center and Lund Stem Cell Center, Lund University, BMC A11, 221 84, Lund, Sweden
5 Institute of Reconstructive Neurobiology, Life and Brain Center, University of Bonn, and German Center for Neurodegenerative Diseases (DZNE), Sigmund-Freud-Straße 25, D-53127, Bonn, Germany

Correspondence to: Zaal Kokaia PhD
Lund Stem Cell Center, University Hospital,
BMC B10,
SE-221 84 Lund, Sweden
E-mail: zaal.kokaia@med.lu.se

Keywords: stem cells; stroke; synapses; transplantation; functional integration

Abbreviations: dMCAO = distal middle cerebral artery occlusion; iPSC = induced pluripotent stem cell; lt-NES = long-term self-renewing neuroepithelial-like stem

Received October 11, 2016. Revised November 2, 2016. Accepted November 20, 2016. Advance Access publication January 22, 2017

Introduction

Stem cell-based approaches hold much promise as potential novel treatments to restore brain function after ischaemic stroke (George and Steinberg, 2015). Transplantation of stem cells or their progeny can improve behavioural impairments in animal models of stroke (Lindvall and Kokaia, 2011). Several possible mechanisms underlying these improvements have been proposed including neuronal replacement, modulation of inflammation, trophic action, and stimulation of plasticity (Kokaia *et al.*, 2012). Although incorporation of stem cell-derived neurons into host neural circuitry will most likely lead to optimum functional recovery after stroke, evidence that neuronal replacement occurs is virtually lacking. It requires the formation not only of efferent projections to the appropriate targets but also establishment of functional synaptic inputs on the stem cell-derived neurons in order to allow for host brain control of neuronal activity in the graft.

Some experimental evidence suggests that grafted stem cell-derived neurons can receive synaptic inputs from the stroke-injured brain. Transplanted neurons, derived from mouse or human neural stem cells (NSCs) or human embryonic stem cells, have been reported to be surrounded by structures expressing synaptic markers and to exhibit spontaneous activity (Buhnemann *et al.*, 2006; Daadi *et al.*, 2009). Some ultrastructural data indicate synaptic connections between host axon terminals and grafted neurons (Daadi *et al.*, 2009; Muneton-Gomez *et al.*, 2012). Intracortically grafted neurons, generated from induced pluripotent stem cells (iPSCs) and differentiated to a cortical phenotype, were found to provide efferent projections to cortical and subcortical areas and to exhibit spontaneous excitatory postsynaptic currents (Tornero *et al.*, 2013). Circumstantial evidence suggested that host neurons had established afferent synaptic contacts on grafted cells (Tornero *et al.*, 2013). Taken together, experimental data demonstrating that transplanted neurons receive synaptic inputs from stroke-injured host brain are scarce, and the origins of afferents and their possible functionality are unknown.

The recently developed rabies virus-based tracing method allows retrograde monosynaptic tracing, unambiguously identifying cells directly presynaptic to postsynaptic neurons (Wickersham *et al.*, 2007). This method has been used to map, e.g. afferent synaptic inputs to adult-born neurons in the dentate gyrus and olfactory bulb (Vivar *et al.*, 2012; Deshpande *et al.*, 2013), and to intrastriatal grafts of human embryonic stem cell-derived dopaminergic neurons (Grealish *et al.*, 2015). Here we have used the trans-synaptic method in combination with immunoelectron microscopy to analyse the afferent synaptic inputs to human iPSC-derived, cortically fated neurons after transplantation to a homotopic site, i.e. the cerebral cortex. Electron microscopy in combination with immunostaining allows the visualization of grafted cells at the ultrastructural level, and thus discrimination of presynaptic and postsynaptic structures (Lepore *et al.*, 2006; Tsupykov *et al.*, 2014). To test the functionality of synaptic inputs to grafted neurons, we have used two approaches: First, physiological sensory stimulation and *in vivo* electrophysiological recordings of spino-(or trigemino)-thalamo-cortical inputs to the transplants. Second, whole-cell patch-clamp recordings from grafted cortical neurons during photostimulation of virally transfected, channelrhodopsin-2-expressing preterminal thalamo-cortical axons in acute brain slices (Yamawaki *et al.*, 2016).

Our results show, for the first time, that intracortically grafted human iPSC-derived cortically fated neurons in the stroke-injured brain receive direct synaptic inputs from neurons in diverse brain areas in a pattern similar to that of endogenous cortical neurons with the same location in the intact brain. We demonstrate that at least some of these afferent inputs are functional, and that physiological sensory stimuli can evoke spikes or inhibit spontaneous activity in the grafted human iPSC-derived cortically fated neurons.

Materials and methods

Animals

All procedures were conducted in accordance with the European Union Directive (2010/63/EU) and were approved by the ethical committee for the use of laboratory animals at Lund University and the Swedish Board of Agriculture. Adult male (225–250 g) Sprague-Dawley rats ($n = 40$; Charles River) were used for short-term experiments (2 month time point). Naïve weight-matched (490–520 g) adult male Sprague-Dawley rats ($n = 5$; Janvier labs) were used as controls in electrophysiological recordings. They were housed in standard caging under a 12-h light/dark cycle with *ad libitum* access to food and water. Adult male (220 g) athymic, nude rats ($n = 16$; Charles River) were used for long-term experiments (6 month time point). They were housed as described above but in individual ventilated cages.

Cell line and cortical priming

Human iPSC-derived long-term neuroepithelial-like (lt-NES) cells were produced from skin fibroblasts as previously described (Koch *et al.*, 2009) and detailed in the Supplementary material. The lt-NES cells were primed towards a cortical neuronal phenotype according to Tornero *et al.* (2013). Growth factors (FGF, EGF) and B27 were omitted and cells were cultured at low density in differentiation-defined medium in the presence of BMP4 (10 ng/ml), Wnt3A (10 ng/ml) and cyclopamine (1 μM) for 7 days. Neuronal progenitors were then dissociated using trypsin and prepared for transplantation.

Lentivirus production and transduction

The construct for the tracing vector was purchased from AddGene (ID: 30195). High-titre preparations of lentiviral par-

ticles were produced according to protocol from Dull *et al.* (1998) in a biosafety level 2 environment. The lt-NES cells were stably transduced with 10% of lentiviral tracing vector during 48 h and checked 1 week later under inverted fluorescence microscope (Olympus) for nuclear GFP expression. The efficiency of transduction was ~80%.

Distal middle cerebral artery occlusion and cell transplantation

Focal ischaemic injury in cerebral cortex was induced as described previously (Supplementary material). Intracortical transplantation of lt-NES cells, which had been transduced with lentivirus carrying GFP (for immunoelectron microscopy and electrophysiological *in vivo* and optogenetic experiments) or with tracing vector (for monosynaptic tracing experiments), was performed stereotaxically at 48 h after distal middle cerebral artery occlusion (dMCAO). On the day of surgery, cortically primed cells in the seventh day of differentiation were resuspended to a final concentration of 100 000 cells/µl. A volume of 1.5 µl was injected at two sites at the following coordinates (from bregma and brain surface): anterior/posterior: +1.5 mm; medial/lateral: −1.5 mm; dorsal/ventral: −2.0 mm; and anterior/posterior: +0.5 mm; medial/lateral: −1.5 mm; dorsal/ventral: −2.5 mm. Tooth bar was set at −3.3 mm. Sprague-Dawley rats were given Cyclosporine A 10 mg/kg subcutaneously every day during the first month and every other day during the second month after transplantation.

Immunoelectron microscopy

Fixed brains were removed, cryoprotected, sectioned, and stained to detect GFP. Sections of transplanted cortex were then processed for electron microscopy. Synapses were defined by the presence of at least two to three synaptic vesicles in a presynaptic terminal, postsynaptic density in postsynaptic structure, and a synaptic cleft. Detailed description is found in the Supplementary material.

ΔG-Rabies vector production and injection

Pseudo-typed rabies vector was produced as previously described (Osakada and Callaway, 2013) with minor adjustments. The protocol was stopped after step 60 as the virus was concentrated via ultracentrifugation only once and no sucrose cushion was used. Titring was performed using TVA-expressing HEK 293 T cells as defined in the protocol. Titres were 20–30 × 10^6 TU/ml. For *in vivo* experiments, we used a dilution of 5%, as determined by testing different dilutions for a concentration that gave specific infection and tracing, in the absence of toxicity. At 2 or 6 months after cell transplantation, intracortical ΔG-rabies vector injection was performed stereotaxically at the following coordinates (from bregma and brain surface): anterior/posterior: +0.5 mm; medial/lateral: −2.5 mm; dorsal/ventral: −2.5 and 1.5 mm; anterior/posterior: +0.7 mm; medial/lateral: −2.9 mm; dorsal/ventral: −2.5 and 1.5 mm; and anterior/posterior: +0.4 mm; medial/lateral: −2.7 mm; dorsal/ventral: −2.5 and 1.5 mm. Tooth bar was set at −3.3 mm. A volume of 1 µl was injected at three sites with two deposits in each (6 µl of 5% ΔG-rabies vector in total). For control experiments, intact rats were injected in the same way with lentiviral tracing vector and 1 week later with ΔG-rabies vector. Animals were sacrificed 1 week later.

Immunohistochemistry

Animals were perfused transcardially with 4% paraformaldehyde. Coronal sections (40 µm) were preincubated in blocking solution (5% normal donkey serum and 0.25% Triton™ X-100 in 0.1 M potassium-buffered saline) and then incubated at +4°C overnight with primary antibodies (Supplementary Table 1) diluted in blocking solution. Fluorophore-conjugated secondary antibodies (Molecular Probes or Jackson Laboratories) were diluted in blocking solutions and applied for 2 h at room temperature, followed by three rinses with potassium-buffered saline. Nuclei were stained with Hoechst 33342 (Molecular Probes or Jackson Laboratories) for 10 min followed by three rinses and sections were mounted with Dabco (Sigma) on gelatin-coated slides. Images were obtained using epifluorescence (Olympus) and confocal (Zeiss) microscopes. For 3D reconstruction of the grafts, area covered by transplanted cells was delineated using human specific marker SC101 and GFP immunostainings. Coronal sections were assembled using cinema 4D software (Maxon).

In vivo electrophysiological recordings and sensory stimulation

Rats were anaesthetized and placed in a stereotactic frame. *In vivo* neuronal activity in response to tactile stimulation was recorded and analysed as described in the Supplementary material.

Optogenetic activation in slices

Channelrhodopsin-2 (ChR2) was expressed in neurons in ventral thalamic nuclei using stereotaxic injections of adeno-associated virus with the plasmid AAV5-hSyn-hChR2(H134R)-EYFP in isoflurane-anaesthetized rats at the following coordinates (from bregma and brain surface): anterior/posterior: −3.0 mm; medial/lateral: −2.7 mm; dorsal/ventral: −5.8 mm. Tooth bar was set at −3.3 mm. A volume of 1.5 µl was injected. At least 10 days following virus injection, coronal brain slices were prepared (Oki *et al.*, 2012). Slices were constantly perfused with carbogenated artificial CSF (in mM: 119 NaCl, 2.5 KCl, 1.3 $MgSO_4$, 2.5 $CaCl_2$, 26 $NaHCO_3$, 1.25 NaH_2PO_4, and 11 glucose, pH ~7.4) at +34°C. Recording pipettes were filled with intracellular solution (in mM: 122.5 potassium gluconate, 12.5 KCl, 10 HEPES, 2.0 MgATP, 0.3 Na_2-GTP, and 8.0 NaCl). Biocytin (1–3 mg/ml) was dissolved in the pipette solution for *post hoc* identification of recorded cells. Grafted GFP-positive cells were identified by autofluorescence, and infrared differential interference contrast microscopy was used when approaching recording pipette to target cell. Whole-cell patch-clamp recordings were performed with EPC10 amplifier using PatchMaster (HEKA) for data acquisition. Cells were held in voltage-clamp at −70 mV. Photostimulation was elicited by pulses of blue light (LED-460 nm, Prizmatix) lasting 5 ms applied through a water

immersion objective (Olympus, 40×/0.8) with a maximum power density of ~1 mW/mm^2. Data were analysed offline with FitMaster (HEKA), IgorPro and NeuroMatic (Wavemetrics).

Results

Host neurons establish afferent synapses with intracortically grafted cortical neurons derived from human iPSCs

In our previous study (Tornero *et al.*, 2013), we showed that at 2 months after intracortical transplantation of human iPSC-derived neuronal precursors in the rat cortical stroke model, about one-fifth of grafted cells expressed the mature neuronal marker NeuN and close to 80% the immature neuronal marker HuD. Grafted cells exhibited pyramidal morphology and expressed cortex-specific neuronal markers. At 5 months, electrophysiological recordings demonstrated grafted cells with the properties of mature neurons. Also at this time point, a considerable percentage of the grafted cells (30.2 ± 0.7%) expressed NeuN, while the majority (77.9 ± 5.4%) expressed HuD (unpublished results).

Here we first wanted to explore using immunoelectron microscopy whether the intracortically grafted human iPSC-derived neurons received synaptic inputs from the stroke-injured host brain. We subjected rats to dMCAO and 48 h later, cortically fated GFP+ lt-NES cells (Tornero *et al.*, 2013) were implanted adjacent to the injury in somatosensory cortex. After 6 months, animals were sacrificed and sections through the cortex were analysed using immunoelectron microscopy using anti-GFP antibodies and DAB-reaction to detect GFP+ neurons and their dendrites with spines and synaptic contacts. The GFP+ lt-NES cell-derived grafted neurons were easily identified due to the intense black electron dense DAB-reaction product within their cytoplasm and processes, whereas the nucleus and mitochondria were DAB− (Fig. 1).

The majority of grafted GFP+ cells exhibited the ultrastructural features of mature neurons, such as round euchromatic nuclei with nucleoli and cytoplasm that was rich in mitochondria, rough endoplasmic reticulum, Golgi apparatus and contained a large number of free ribosomes (Fig. 1A). In addition, we observed a small population of GFP+ astrocytes with bundles of intermediate filaments and glycogen granules (data not shown). GFP− host axon terminals formed synaptic contacts on most of the GFP+ grafted neurons, showing all of the ultrastructural criteria for synapses, which require clustering of synaptic vesicles close to presynaptic membrane, synaptic cleft containing intermediate layer of dense material and postsynaptic membrane with evident postsynaptic densities (Fig. 1B–E).

The ultrastructure of these synaptic contacts was indistinguishable from that of synapses in the host somatosensory cortex. We classified synaptic contacts between grafted and host neurons according to the type of synaptic specialization (asymmetric, symmetric) and the postsynaptic element (cell soma, dendritic shaft, spine). A total of 204 labelled synapses from four rats were analysed. The grafted neurons formed a range of synaptic contacts, afferent inputs being predominant (78.5%) compared to efferent outputs (21.5%) (Fig. 1C). The overall majority (91.6%) of afferent synaptic contacts were axodendritic and only 8.4% were axosomatic (Fig. 1C). Among axodendritic synaptic contacts, 84.7% of axon terminals were in contact with GFP+ dendritic spines, identified on the basis of shape, size and presence of a spiny apparatus (Fig. 1D and E). This type of synaptic contacts prevails in the mammalian cortex (Harris and Kater, 1994). Other host axons terminated on dendritic shafts (11.1%) or on structures that were either small shafts or dendritic spines (4.2%). All axodendritic contacts were asymmetric with structural characteristics of excitatory/glutamatergic synapses, such as a prominent postsynaptic density, wide synaptic cleft and spherical synaptic vesicles (Fig. 1D and E). Most postsynaptic densities (94.3%) were non-perforated (simple) and only 5.7% were perforated. The host axon terminals displayed abundant synaptic vesicles, and particularly docked vesicles at the presynaptic membrane (Fig. 1D and E), suggesting the presence of a readily releasable pool of synaptic vesicles. These ultrastructural signs indicate functional activity of synapses (Schneggenburger *et al.*, 2002).

Taken together, our ultrastructural data show that the grafted human iPSC-derived cortical neurons receive afferent inputs from the stroke-injured host brain, forming excitatory axodendritic synaptic contacts similar to those observed in other parts of the somatosensory cortex.

Human iPSCs-derived intracortically grafted cortical neurons receive direct synaptic inputs from normal pattern of host brain areas

We then wanted to determine the origins of afferent synaptic inputs from stroke-injured host brain to grafted cells. For this purpose, we used a modified rabies virus (ΔG-rabies), in which the gene for glycoprotein is replaced by the gene for the fluorescent protein mCherry in the viral genome. The envelope is substituted with the foreign coat protein EnvA, generating replication-incompetent virus that only can infect cells expressing the TVA receptor (Supplementary Fig. 1A). Human iPSC-derived lt-NES cells were transduced to stably express glycoprotein, avian TVA receptor and histone-GFP under control of the human synapsin I promoter (tracing vector, Supplementary Fig. 1B).

Eight rats were subjected to dMCAO and 48 h later, cortically fated lt-NES cells transduced with lentiviral

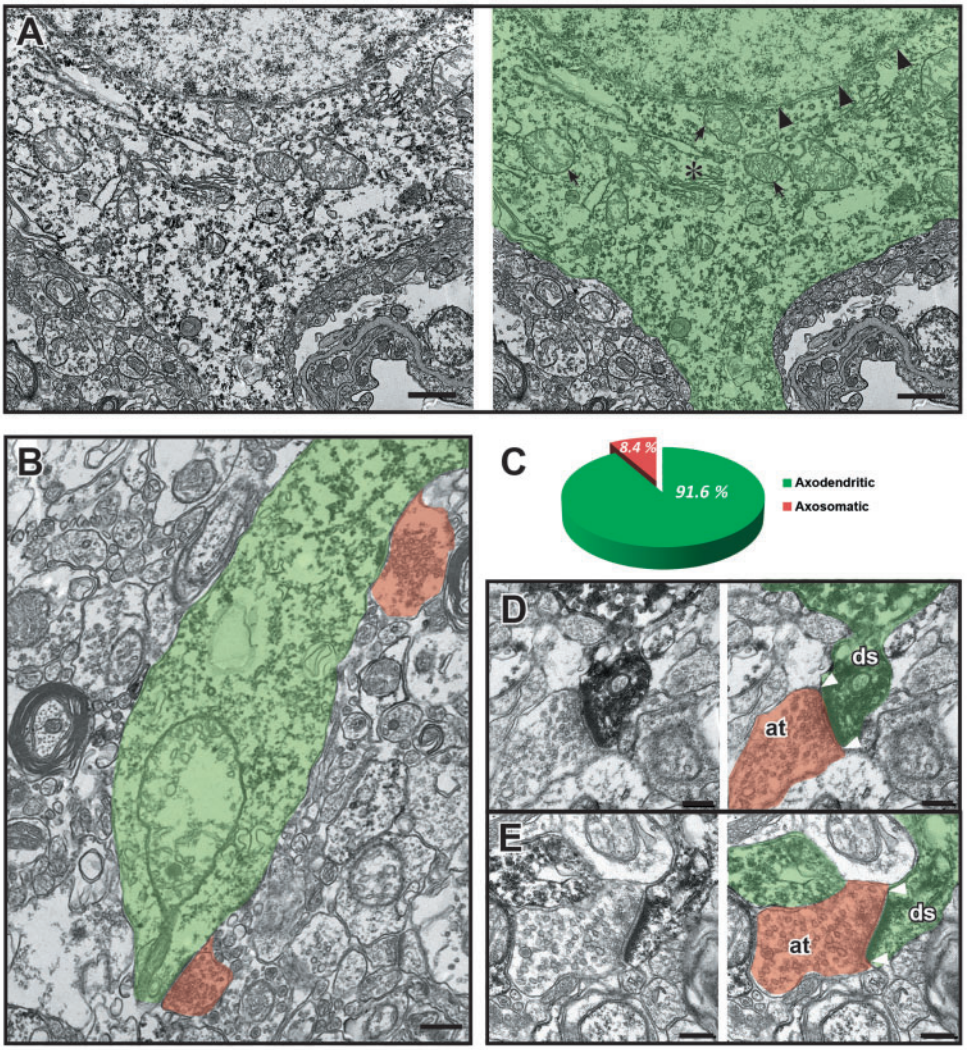

Figure 1 Host neurons establish afferent synapses with grafted cortical neurons derived from human iPSCs. (**A**) Grafted GFP/DAB + neuron (marked in green on *right* image) with DAB− nucleus (arrowheads) and mitochondria (arrows). The grafted neurons are rich in rough endoplasmic reticulum, Golgi apparatus (asterisk) and mitochondria. Scale bar = 0.5 μm. (**B**) Host axon terminals (marked in red) which have established afferent synaptic contacts with grafted GFP/DAB + neuron (green). Scale bar = 0.2 μm. (**C**) Proportions of GFP/DAB + synaptic axodendritic versus axosomatic contacts. (**D** and **E**) Asymmetric synapses with continuous postsynaptic densities (white arrowheads) in grafted GFP/DAB + (green) dendritic spines (ds) connected with host presynaptic axon terminals (at, red). Scale bar = 0.2 μm.

tracing vector were implanted adjacent to the injury in somatosensory cortex. After 2 months, ΔG-rabies vector was injected at the location of the graft (Tornero *et al.*, 2013) and animals were perfused 7 days thereafter (Supplementary Fig. 1C). Since expression of the TVA receptor in mature, synapsin I-positive neurons, generated from the grafted cells makes them susceptible for infection with ΔG-rabies vector, presence of glycoprotein in these cells allows the virus to infect cells that are connected to them by functional synapses. Therefore, grafted and infected cells will express nuclear GFP and cytoplasmic mCherry (starter neurons), whereas the ones monosynaptically connected to them will only express mCherry in their cytoplasm (traced neurons) (Supplementary Fig. 1D). Further propagation of the ΔG-rabies vector is not possible as expression of glycoprotein is restricted to the starter neuron (Etessami *et al.*, 2000).

The ischaemic lesion was confined to somatosensory cortex and grafted cells, which expressed nuclear GFP at high percentage (~80%), had survived in large numbers (Fig. 2A). Starter neurons (GFP + /mCherry +) were easily distinguishable from traced neurons (GFP−/mCherry +) (arrowheads and arrows, respectively, in Fig. 2B). We estimated that 20–90% of GFP + neurons were starter neurons (mCherry +) in the different grafts. Immunostaining using human specific antibodies (SC101 and SC121) confirmed the discrimination between grafted human neurons not transduced with tracing vector and traced host rat neurons in the close vicinity of the transplant (Fig. 2B).

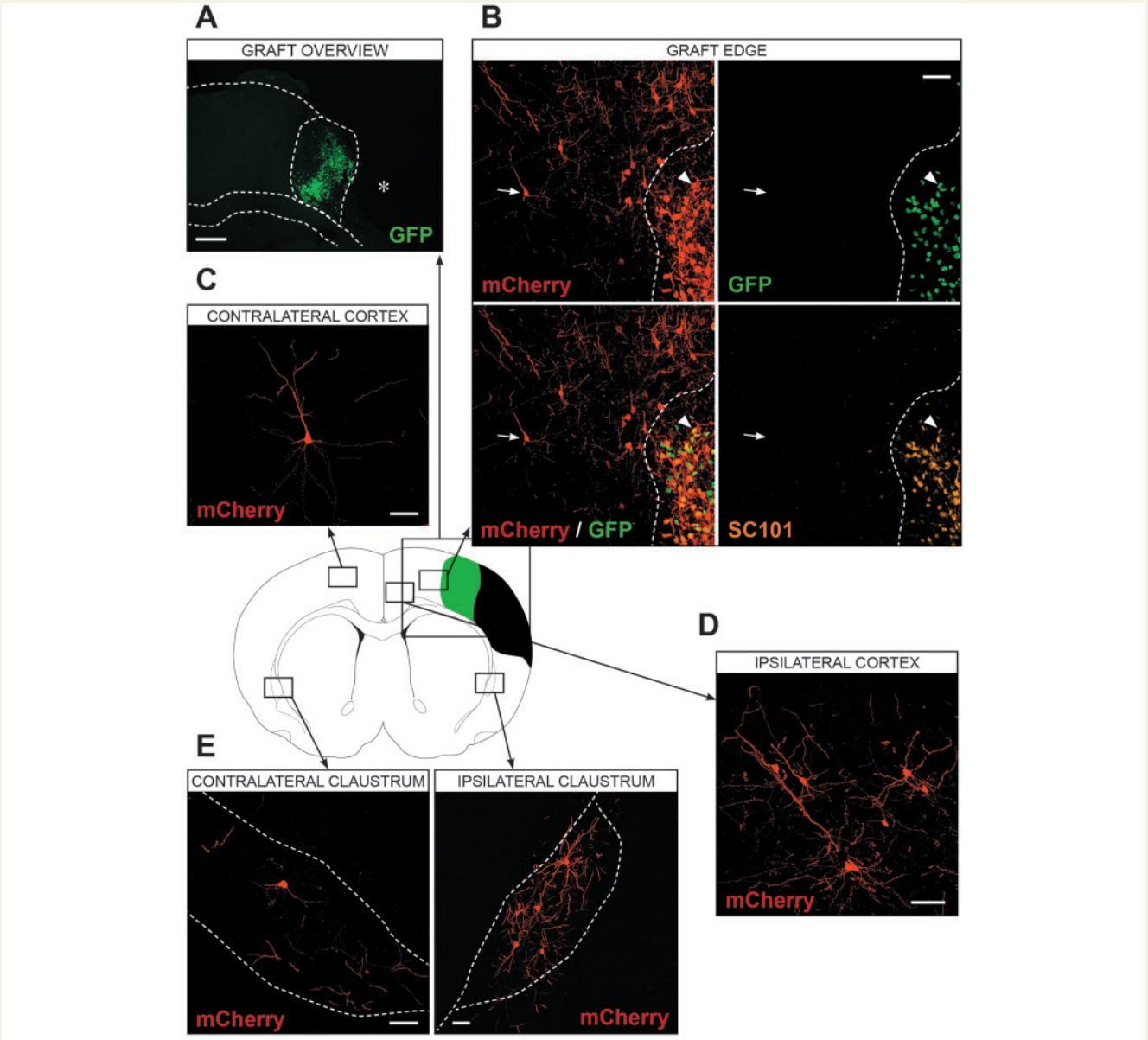

Figure 2 Grafted cortical neurons derived from human iPSCs receive direct synaptic inputs from host neurons in cortical areas. Fluorescence photomicrographs showing location of starter and traced neurons in cerebral cortex using rabies virus monosynaptic tracing at two months after stroke and intracortical transplantation of human iPSC-derived cortical neurons. (**A**) Overview of the graft stained for GFP, present in nuclei of the cells expressing tracing vector. Edge of the cortex, corpus callosum and graft are highlighted with dotted line. Asterisk indicates stroke cavity. Scale bar = 500 μm. (**B**) Edge of the graft stained for GFP (green), mCherry (red) and human-specific nuclear marker SC101 (orange). Graft border is highlighted with dotted line. Starter neurons (GFP + /mCherry + ; arrowheads) are easily distinguishable from traced neurons (GFP−/mCherry + ; arrows). Immunostaining using human specific antibody (SC101) is used to confirm location of grafted cells. Scale bar = 50 μm. (**C–E**) Traced host neurons in the contralateral cortex (**C**), ipsilateral cortex (**D**) and claustrum of both hemispheres (highlighted with dotted lines; **E**). Scale bars = 50 μm.

Immunohistochemical analysis at 2 months after transplantation revealed the presence of GFP−/mCherry + traced neurons in diverse areas of stroke-injured brain (Table 1, and Figs 2 and 3). The cortical area adjacent to the graft showed high density of traced neurons with various morphologies and random distribution in different layers (Fig. 2B and D). Most traced neurons were immunopositive for the glutamatergic marker KGA and some of them expressed calretinin (Supplementary Fig. 2A and B). The density of traced neurons in ipsilateral cortex tapered off when moving away from the graft. In contralateral cortex, traced neurons were accumulated in the area corresponding to the location of the graft (Fig. 2C). These neurons were located in layers 2/3 and 5, had pyramidal

Table 1 Relative numbers of traced neurons in different areas of stroke-injured, transplanted brain or intact brain following injection of modified rabies virus vector in the graft or corresponding cortical area

Area/nucleus	Stroke + graft	Intact
Cortex		
Cortex ipsilateral	+ + +	+ + +
Cortex contralateral	+ +	+ +
Claustrum ipsilateral	+ +	+ +
Claustrum contralateral	+	+ +
Thalamus		
Ventral posterolateral	+ +	+ +
Ventrolateral	+ +	+ +
Ventromedial	+ +	+ +
Ventral posteromedial	+ +	+ +
Ventral anterior	+	+ +
Anteroventral ventrolateral	0	+
Anterodorsal	0	+
Anteromedial ventral	0	+
Anteroventral	0	+
Laterodorsal dorsomedial	+	+
Laterodorsal ventrolateral	0	+
Lateroposterior mediorostral	0	+
Posterior	+	+ +
Others		
Globus pallidus lateral	+	+ +
Globus pallidus medial	+	+
Basolateral amygdala	+	+
Hippocampus CA1	+	+
Lateral hypothalamic area	+	+

Semiquantitative representation of relative numbers of traced cells as calculated by dividing the actual number of counted cells in each area with the total number of starter neurons in each brain. The relative numbers are shown as follows: No detectable cells, 0; >0–1 cells, + (low); >1–50 cells, + + (medium); and >50 cells, + + + (high). Terminology according to Paxinos and Watson (1998).

morphology, and were KGA+ (Supplementary Fig. 2B). We found high density of traced host neurons bilaterally in dorsal claustrum, especially on the ipsilateral side (Fig. 2E). All these neurons were KGA+ (Supplementary Fig. 2C).

A large number of traced host neurons were detected in thalamus. Highest density was found in ventral and posterior nuclei (Table 1 and Fig. 3); just a few were present in laterodorsal nuclei (particularly in dorsomedial nucleus), and none were found in anterior nuclei or reticular nucleus (Fig. 3A and B). Traced neurons in thalamus had oval cell bodies and multipolar dendritic trees (Fig. 3B and C). About 20% of mCherry+ traced neurons were calbindin+ and calretinin+, and 60% were KGA+ (Supplementary Fig. 2D–F), whereas parvalbumin+ traced neurons were not found.

We observed a few traced neurons in areas outside cortex and thalamus such as globus palidus, basolateral amygdala and lateral hypothalamic nucleus. Single cells were detected in hippocampal CA1 layer, raphe area and brainstem (Table 1).

To determine whether the direct synaptic inputs from stroke-injured brain to grafted neurons underwent changes at longer time points, eight rats were subjected to dMCAO and transplanted 48 h thereafter with cortically fated lt-NES cells transduced with lentiviral tracing vector prior to differentiation. After 6 months, we injected ΔG-rabies vector at the location of the graft and the animals were perfused 7 days later. We found no differences either in number or distributional pattern of traced host neurons as compared to the 2 month time point (Supplementary Fig. 3). In agreement with our findings, Grealish *et al.* (2015) found that the host brain connectivity with human embryonic stem cell-derived neurons in intrastriatal grafts, as shown with rabies virus tracing, was stable between 6 weeks and 6 months after transplantation.

The distribution of the traced host neurons seemed to correspond with the proper anatomical locations of neurons projecting to the somatosensory cortex in the intact brain, where the lesion and the graft were located (Hur and Zaborszky, 2005; Fame *et al.*, 2011; Leisman and Melillo, 2013; Liang *et al.*, 2013; Zakiewicz *et al.*, 2014). To confirm this, we infected six intact rats with lentiviral tracing vector and 1 week later with the ΔG-rabies vector at the same coordinates as used for targeting the graft (Supplementary Fig. 1E). Importantly, analysis of the brains 1 week later showed the presence of traced neurons in the same areas where we had found traced neurons in the transplanted stroke-damaged animals (Supplementary Fig. 4 and Table 1).

Intracortically grafted cortical neurons derived from human iPSCs are activated by physiological sensory stimuli

We wanted to determine whether the direct synaptic inputs to grafted neurons were functional, i.e. causing excitatory effects strong enough to elicit spikes or inhibitory effects on ongoing spontaneous activity. In the intact brain, sensory information from the body is mediated to primary somatosensory cortex through thalamocortical pathways including the ventrobasal and intralaminar nuclei. To explore whether the grafted cells respond to sensory input, we subjected 10 rats to dMCAO and transplanted them 48 h later with GFP-lt-NES cells in the cortical area adjacent to the injury. Three months later, electrophysiological activity was recorded extracellularly from neurons in the grafted tissue in anaesthetized animals ($n = 4$) while tactile stimulation of different areas of the body was performed. Care was taken to obtain high quality recordings from the central part of the grafts as originally estimated from UV photos of the cortical surface (Fig. 4A and B). We set the following criteria to include only signals originating from grafted neurons: (i) minimum distance of 70 μm to the border of the graft as defined by post-mortem 3D-immunohistochemistry; and (ii) spike amplitude of >100 μV and signal to noise ratio of >2.5 (Buzsaki, 2004; Thorbergsson *et al.*, 2012).

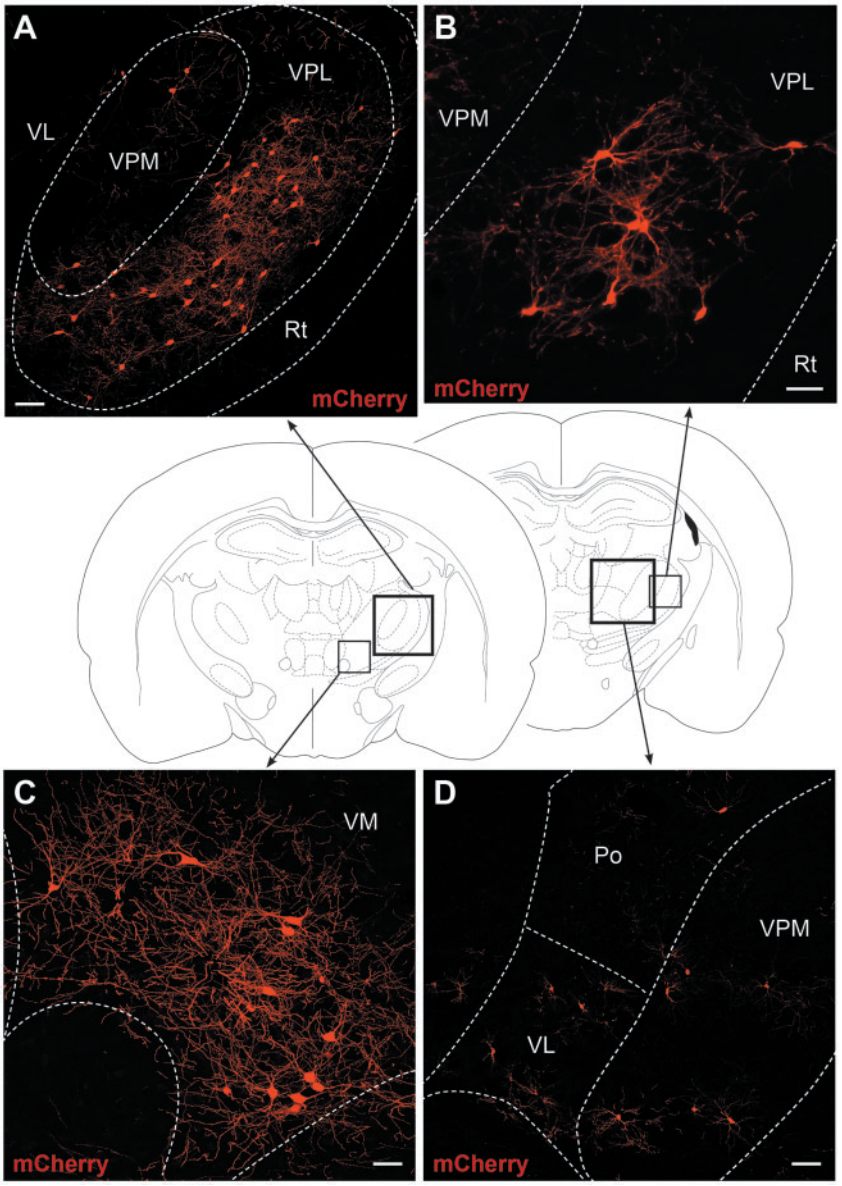

Figure 3 Grafted cortical neurons derived from human iPS cells receive direct synaptic inputs from host neurons in thalamic nuclei. Fluorescence photomicrographs showing location of traced neurons in thalamic nuclei using rabies virus monosynaptic tracing at 2 months after stroke and intracortical transplantation of human iPSC-derived cortical neurons. (**A–D**) Traced host neurons (mCherry+) in ventral posterolateral nucleus (VPL; **A** and **B**), ventromedial nucleus (VM; **C**), ventral posteromedial nucleus (VPM; **A** and **D**), ventrolateral nucleus (VL; **D**) and posterior nucleus (Po; **D**). Note the absence of traced neurons in reticular nucleus (Rt; **A** and **B**). Dotted lines highlight relevant structures. Scale bars = 100 μm (**A** and **D**) and 50 μm (**B** and **C**).

Five naive rats were used as controls. We also obtained recordings from somatosensory cortex adjacent to the ischaemic lesion in two rats with no surviving grafted cells.

Ten unit recordings in the grafts fulfilled the inclusion criteria (Table 2). The neurons were recorded at a depth below the surface ranging from 700 to 1250 μm. All but one of these neurons received a short latency (within the first 50 ms from stimulation onset) excitatory input from the nose with onset latency ranging from 9 to 32 ms. Four neurons received an additional short latency excitatory input from either of the ipsilateral forepaw, the contralateral forepaw, the ipsilateral hindpaw or the contralateral hindpaw. Spontaneous activity in four neurons was inhibited by tactile stimulation of at least one body area with an onset latency of between 46 and 85 ms. Figure 4 shows a representative example of a neuron (recording number 4 in Table 2 and electrode position number 3 in Supplementary Table 2) that responded to tactile stimulation of the nose with a latency of 32 ms followed by a period of inhibition of spontaneous activity, while stimulation of the ipsilateral forelimb resulted only in short latency inhibition of spontaneous activity.

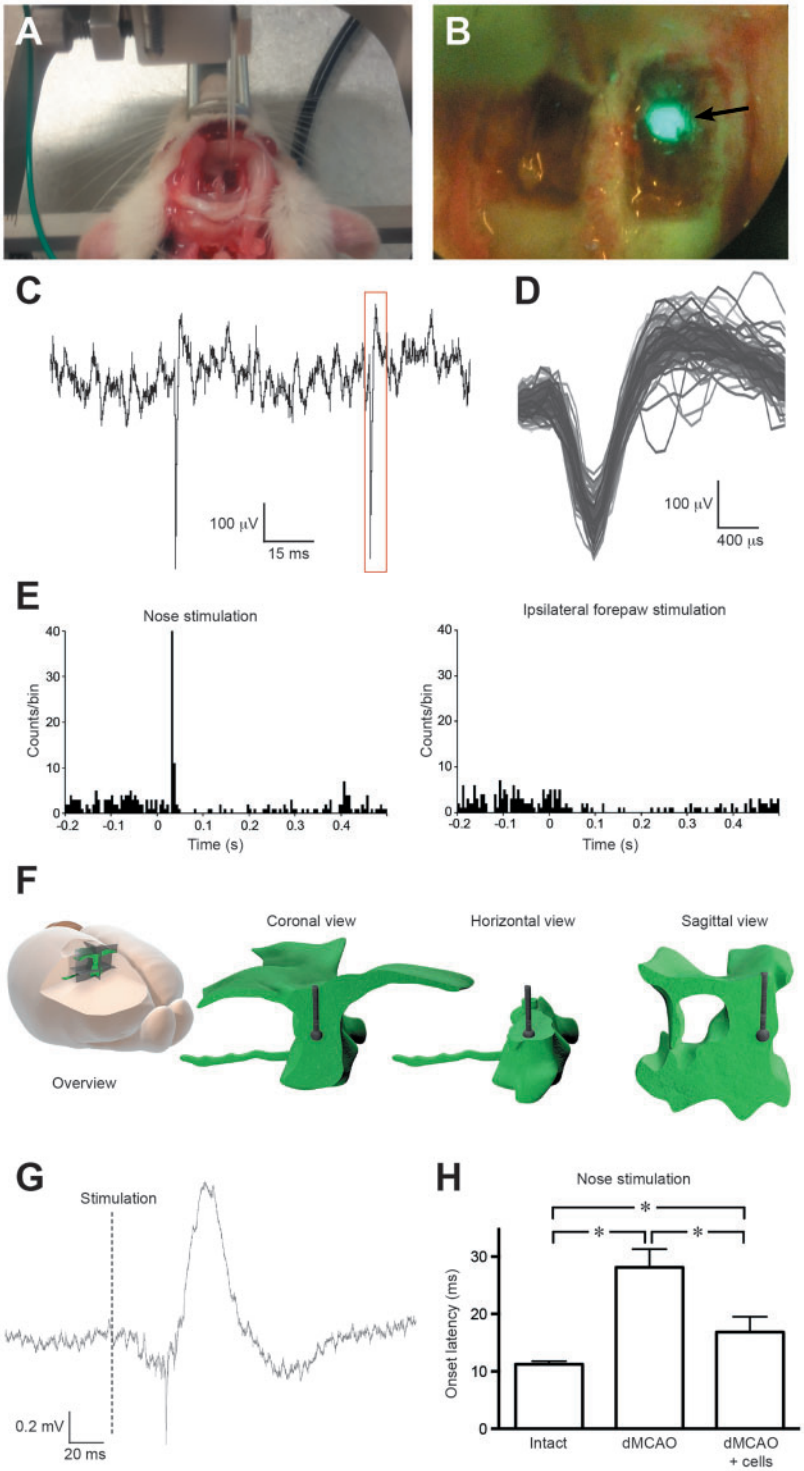

Figure 4 Intracortically grafted cortical neurons derived from human iPS cells are activated by physiological sensory stimuli. (**A**) Overview of the set-up used for *in vivo* electrophysiological recordings. Two squared windows in the skull were produced to expose somatosensory cortex. (**B**) Photograph showing the view of the graft through the dissection microscope under UV illumination. Arrow points the location of the graft (GFP + area) in the right hemisphere of the brain. (**C**) One example of unfiltered spontaneous neuronal activity. (**D**) Overlaid waveforms, highlighted in **A** with red square, from an identified neuron, with increased time scale. (**E**) Peristimulus time histograms from an identified neuron based on responses to 100 tactile stimulations at 1 Hz of the nose (*left*) and ipsilateral forepaw (*right*). Note the different responses depending on stimulation site. (**F**) Coronal, horizontal and sagittal view of 3D reconstruction over the recording site, according to the upper scheme. The green areas are corresponding to neuronal grafted tissue and the black sphere at the end of the capillary indicates a diameter of 100 μm around the recording site of the electrode. (**G**) Example of an evoked potential elicited by tactile stimulation of the nose. Note the neuronal spikes. (**H**) Onset latency for excitatory input evoked by nose stimulation in control animals (intact, $n = 34$ units), animals subjected to dMCAO with no surviving grafted cells (dMCAO, $n = 7$ units), and animals subjected to dMCAO with surviving grafted cells (dMCAO + cells, $n = 7$ units). In the latter group, only units with no host neuron closer than 70 μm from the electrode position are included. Data represent means ± SEM; $^*P < 0.05$, one-way ANOVA *post hoc* test.

Table 2 ***In vivo*** **electrophysiological recordings from grafted cells after peripheral sensory stimulation**

Recording number	Nose	Forepaw		Hindpaw		SNR	Amplitude (μV)
		Contra	Ipsi	Contra	Ipsi		
1	*55*	n.r.	n.r	n.r.	n.r.	9.55	294
2	**12**	n.r.	n.r.	n.r.	n.r.	11.50	369
3	**11**	n.r.	n.r.	**44**	n.r.	3.68	116
4	**32**	n.r.	*50*	n.r.	*78*	10.58	301
5	**16**	n.r.	*51*	*85*	**42**	4.28	102
6	**16**	n.r.	**33**	n.r.	n.r.	20.19	463
7	**9**	n.r.	n.r.	n.r.	n.r.	3.43	110
8	**31**	n.r.	n.r.	n.r.	n.r.	9.97	381
9	**21**	n.r.	n.r.	n.r.	n.r.	2.54	106
10	**13**	**34**	*46*	n.r.	n.r.	5.09	175

Nose, forepaw and hindpaw represent responses to peripheral stimulation in the different areas (Contra = contralateral; Ipsi = ipsilateral; n.r. = no response). Excitatory responses are shown in bold (onset latency in ms). Values in italics represent inhibitory responses (onset latency in ms). SNR = signal to noise ratio. Amplitude = maximum amplitude of the response.

Units ($n = 75$) recorded in forelimb primary somatosensory cortex in naive rats received short latency excitatory tactile input mainly from contralateral forelimb (61% of units), nose (45% of units) and ipsilateral forelimb (25% of units). Inhibitory tactile input was found mainly from contralateral forelimb (24% of units), ipsilateral forelimb (19% of units) and nose (24% of units).

Recordings from the cortical area adjacent to the stroke lesion in two rats with no surviving grafted cells were performed to evaluate the effect of the damage on the response to tactile stimulation. These units ($n = 12$) received an excitatory input mainly from the ipsilateral forelimb (75% of units), nose (58% of units) and contralateral forelimb (33% of units). No inhibitory input was found.

Analysis of the onset latency for excitatory input from the nose in these three groups of animals revealed significant recovery in the recordings from grafted cells as compared with animals with no surviving grafted cells (16.9 ± 7.6 ms and 28.1 ± 8.4 ms, respectively), but not arriving to be complete as in control animals (11.2 ± 3.2 ms) (Fig. 4H).

After recordings had been completed, brains were analysed using immunohistochemistry to show the cellular composition of the transplants and to ensure that the recorded signals originated from grafted neurons. We found that about one-fifth of the lt-NES cells had differentiated to mature NeuN + neurons ($20.6 \pm 1.4\%$ of cells immunoreactive for human-specific SC101 antibody) (Fig. 5A). The majority of these neurons were KGA + ($89.3 \pm 2.7\%$ of NeuN + cells) (Fig. 5B). Mature astrocytes, immunoreactive for human-specific GFAP, were also found in a small percentage ($4.5 \pm 0.5\%$ of SC101 + cells) (Fig. 5C). A high proportion of transplanted cells expressed the immature neuronal marker HuD ($69.9 \pm 5.6\%$ of SC101 + cells) (Fig. 5D).

Immunohistochemical staining against GFP and SC101 (Fig. 5) was used to delineate the area occupied by the grafted cells and served to generate a 3D reconstruction of graft location and morphology. We detected cells of host origin within the area of the transplant, such as microglia and astrocytes ($11.1 \pm 1.7\%$ and $1.6 \pm 0.6\%$ of total number of cells in graft area, respectively; Supplementary Fig. 5A and B). The overall majority of NeuN + mature neurons inside the area of the transplant were grafted cells (SC101 +, $91.8 \pm 3.1\%$ of NeuN + cells), but a small percentage had host origin ($8.1 \pm 2.1\%$ of NeuN + cells), most of them being located in the periphery of the transplant.

We finally made a detailed analysis using microscopy to confirm that the electrophysiological responses originated from grafted neurons and not from the small proportion of host neurons located within the area of the transplant. We determined, in consecutive coronal sections, the location and number of grafted and host neurons in the vicinity of all recording sites (Supplementary Fig. 5C and D). The distance between the closest host neuron and the recording site was measured (Supplementary Table 2 and Supplementary Fig. 5C and D). The overall majority of neurons surrounding the electrodes at the recording sites had graft origin. Only in two of the electrode positions (position 1 and position 4, Supplementary Table 2), we detected a host neuron located closer than 70 μm (69.3 and 22.1 μm, respectively). Thus, it cannot be entirely excluded that recordings were made from host neurons in these positions and, therefore, they were not included in the onset latency analysis (Fig. 4H). However, the lack of any neurons of host origin within 70 μm in the other positions strongly indicates that the electrophysiological responses originated from putative grafted neurons.

Intracortically grafted cortical neurons derived from human iPSCs respond to optogenetic activation of thalamic afferent axons

Finally, we wanted to confirm the functionality of the afferent inputs from ventral thalamic host neurons to the

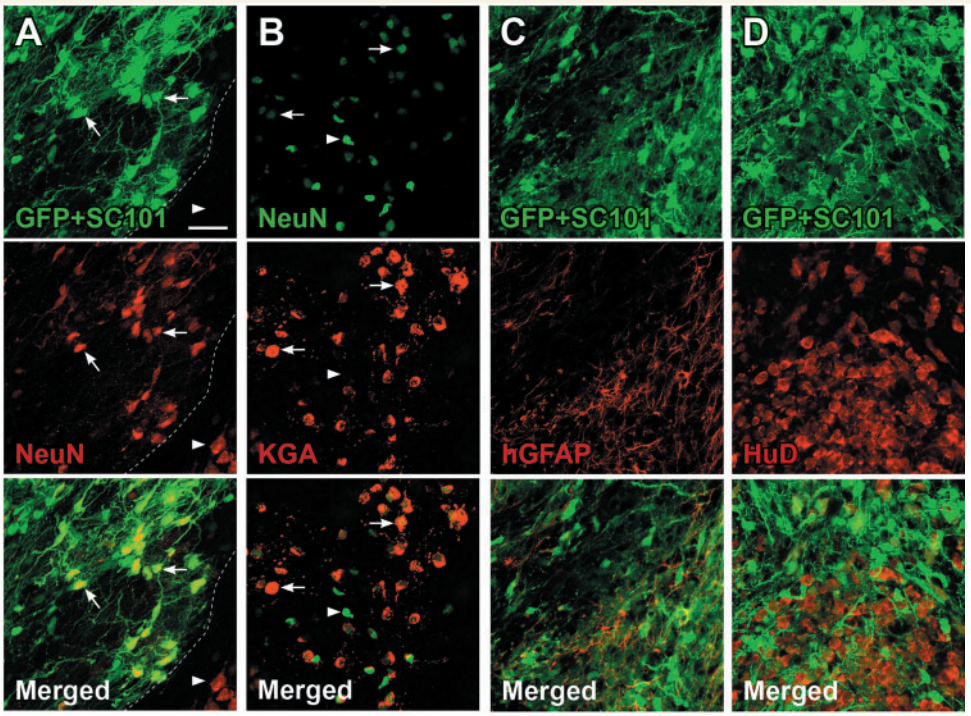

Figure 5 Intracortically grafted cortical precursors predominantly generate excitatory neurons. (**A–D**) Confocal fluorescence photomicrographs showing expression (in red) of NeuN (**A**), KGA (**B**), human specific GFAP (**C**) and HuD (**D**) in grafted cells from recorded transplants, immunostained with the human-specific antibody SC101 and against GPF (green). In (**A**), arrows depict double-positive cells within the graft area delineated by dashed white line, while arrowhead indicates host neuron outside the graft area, immunoreactive only for NeuN. In **B**, the majority of grafted neurons (NeuN+) also express KGA (arrows), while arrowhead depicts a rare NeuN+ but KGA− grafted cell. Scale bar = 40 μm.

intracortically grafted cortical neurons by combining optogenetics and patch-clamp recordings. To test the feasibility of our experimental approach, we first injected four intact rats with ChR2-expressing virus into the ventral nuclei of the thalamus, which contained a high proportion of traced neurons projecting to the grafted neurons or the corresponding somatosensory cortical area in non-grafted animals in monosynaptic tracing experiments (Table 1). Ten days later, we recorded in acute brain slices using patch-clamp from cortical neurons located in somatosensory cortex. Seven out of seven cortical cells responded to photostimulation (Fig. 6A and C). Based on the electrophysiological characteristics of these cells, we distinguished both pyramidal neurons (Fig. 6A) and fast-spiking interneurons (Fig. 6C). Immunostaining of thalamus in the same brains showed many virus-infected, GFP+ neurons in ventral nuclei, including ventral posterolateral, ventrolateral, ventromedial, ventral posteromedial and ventral anterior nuclei (Supplementary Fig. 6C–E). A few GFP+ cells were found in other medial, anterior and posterior nuclei but never outside the thalamus (Supplementary Fig. 6D). Massive numbers of GFP+ axons were found in the slices used for electrophysiological recordings, mainly in somatosensory cortex with higher density in layers 3 and 4 (data not shown).

We then subjected 12 rats to dMCAO and after 48 h they were transplanted intracortically with lt-NES cells expressing GFP. Two months later, the rats were injected with ChR2-expressing virus into ventral thalamic nuclei as above. Between 10 and 34 days after virus injection, we performed patch-clamp recordings from grafted GFP+ cells while photostimulating thalamic preterminal axons, which were massively reaching the somatosensory cortex, including the area of the graft. Of nine recorded cells with neuronal electrophysiological characteristics, two cells responded to light stimulation (Fig. 6B and D). During depolarizing current injections one cell exhibited regular spiking pattern [Fig. 6B(1)], typical of pyramidal neurons, while the other exhibited fast-spiking behaviour [Fig. 6D(1)], typical of a subset of GABAergic interneurons. The majority of non-responding neurons had a pyramidal phenotype. Graft origin was confirmed and morphology of recorded cells, loaded with biocytin, was assessed with immunostaining against GFP in the slices (Fig. 6B and D). Also in this experiment, analysis of the brains demonstrated that virus-infected neurons were confined to thalamic nuclei, particularly ventral ones (Supplementary Fig. 6F). Notably, these neurons showed morphology and distribution similar to what had been observed with the monosynaptically traced cells, projecting to the graft or

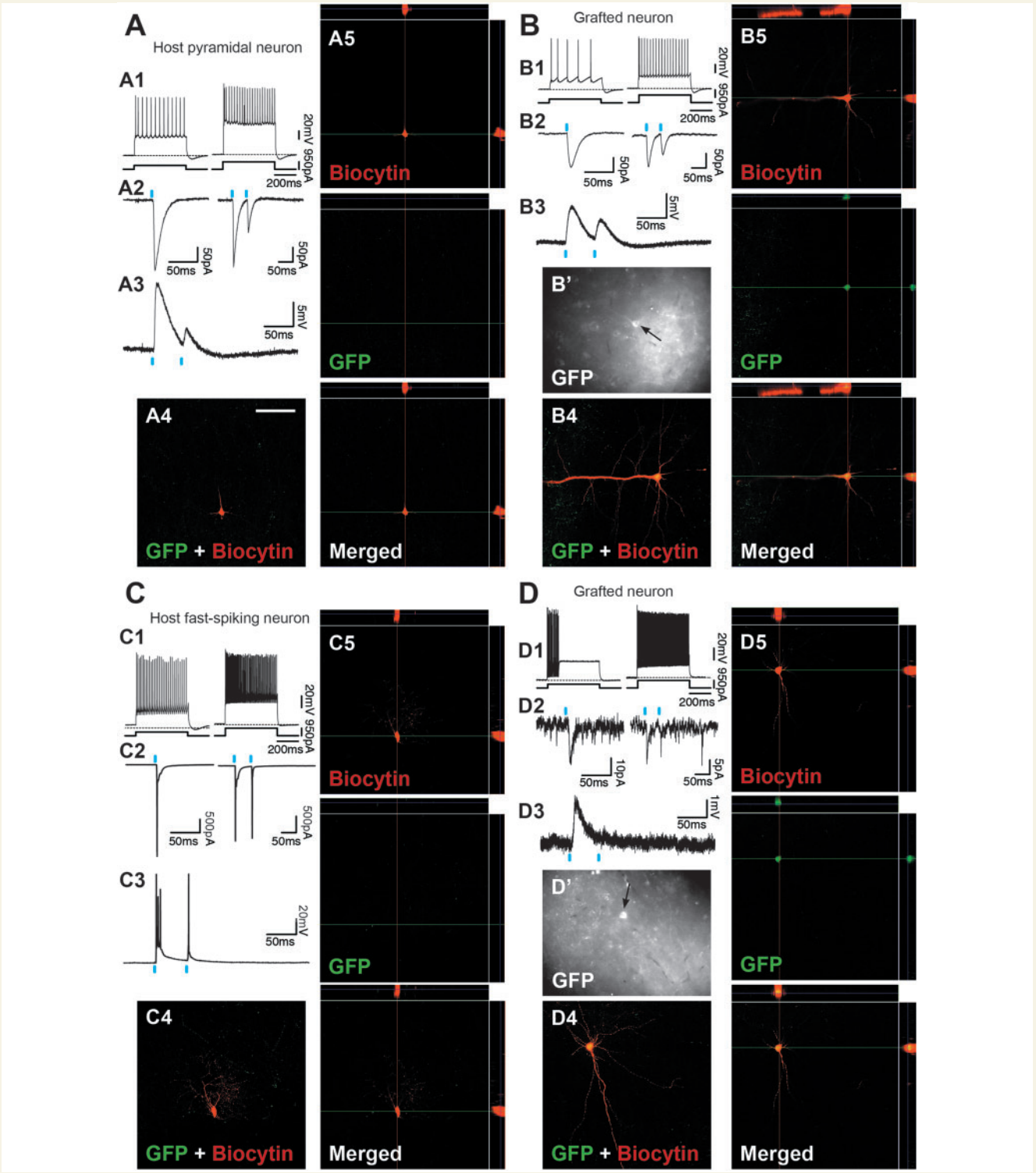

Figure 6 Intracortically grafted cortical neurons respond to optogenetic activation of thalamic afferents. Whole-cell patch-clamp recordings from host (**A** and **C**) and grafted (**B** and **D**) cortical neurons. Current-clamp recordings (**A1–D1**) reveal that the cells are able to generate action potentials upon current injections. Postsynaptic currents (**A2–D2**) and postsynaptic potentials (**A3–D3**) were evoked by photostimulation of ChR2-expressing thalamic afferent axons. Blue bar indicates light illumination (lasting 5 ms). Optimal projection (**A4–D4**) and orthogonal view (**A5–D5**) of fluorescent immunostaining against GFP and biocytin from recorded cell are presented to confirm morphology and graft origin. Recordings from grafted cells also include photomicrograph of GFP autofluorescence under path-clamp microscope (**B'** and **D'**). Arrow depicts recorded cell (corresponding to recordings **B1–3** and **D1–3**, respectively). Recordings show cells with electrophysiological characteristics of both pyramidal neurons (**A** and **B**) and fast-spiking interneurons (**C** and **D**). Scale bar = 100 μm.

corresponding cortical area, in the rabies virus experiment (Fig. 3 and Supplementary Fig. 3 and 4).

Discussion

Here we present four lines of experimental evidence demonstrating, for the first time, that intracortical grafts of adult human iPSC-derived cortically fated neurons receive direct synaptic inputs from stroke-injured brain, and that these afferents are functional. First, we show using immunoelectron microscopy that GFP− host axon terminals form synapses on GFP + grafted neurons, most contacts exhibiting the ultrastructural characteristics of excitatory, glutamatergic synapses. Second, we demonstrate using the rabies virus-based trans-synaptic tracing method that the grafted neurons, localized adjacent to the ischaemic lesion in the somatosensory cortex, receive synaptic inputs from a large number of neurons in ipsi- and contralateral cortex and various thalamic nuclei, as well as from neurons in other forebrain and brain stem areas. We find that the grafted neurons receive afferent inputs from the same areas as endogenous neurons with the same location in the intact brain. Third, we demonstrate using *in vivo* electrophysiological recordings that at least some projections to grafted neurons are functional after sensory stimulation of forepaw, hindpaw and nose, and that these neurons become integrated in host neural circuitry. Finally, we provide further evidence for the functionality of the afferent inputs by showing, using patch-clamp recordings, that a portion of grafted neurons respond to photostimulation of virally transfected, ChR2-expressing thalamo-cortical axons in acute brain slices.

Our findings strongly indicate that the majority of *in vivo* electrophysiological recordings in response to sensory stimulation were made from grafted neurons. Unit recordings, ranging from 102 to 463 μV, were made centrally in the grafts with minimal distance ranging between 70 to 175 μm to the graft border. We found a complete lack of host neurons within 70 μm from several recording sites. It is known that extracellularly recorded action potentials can be discerned from background noise up to about 50 μm from the cell (Buzsaki, 2004; Thorbergsson *et al.*, 2012). It should be noted that this distance applies to the units with the lowest amplitudes. Unit recordings with high amplitudes can only be obtained at a much shorter distance. The grafted neurons received an excitatory tactile input primarily from the nose, and some neurons also from either of the four paws. Inhibition of spontaneous activity by stimulation of paws and nose was also observed. These findings show establishment of functional connections that could elicit action potentials or inhibit spontaneous activity in the grafted neurons in response to physiological stimulation of the skin. The observed convergence patterns and onset latencies of evoked responses in the grafted neurons resemble those found in the naive rats and the previously described input patterns in rat somatosensory cortical areas, in particular in the infralaminar cortex (Tutunculer *et al.*, 2006; Moxon *et al.*, 2008). However, given that the cortical area, where the grafts were placed, normally receives a strong excitatory input from the contralateral forelimb and hindlimb, the relative lack of excitatory input from these body regions indicates that a normal somatotopic organization is not fully restored. Based on our tracing studies, the input to the transplants could be mediated by direct projections of ascending pathways through thalamus (Aguilar *et al.*, 2008) to the grafted neurons (Allison *et al.*, 1989; Kalliomaki *et al.*, 1993), or indirectly via thalamus to contralateral cortex and then via interhemispheric connections through corpus callosum (Kanno *et al.*, 2003), or by pathways through thalamus and then via ipsilateral cortico-cortical connections (Chapin *et al.*, 1987).

So far, only a single study has provided indirect experimental evidence that neural grafts implanted in the stroke-injured brain are able to respond to physiological stimuli through afferent inputs. Grabowski *et al.* (1993) reported that stimulation of the vibrissae region induces higher glucose uptake in intracortical grafts of embryonic cortical tissue in rats with ischaemic cortical lesions. However, findings in other models using intracortical implants of embryonic brain tissue or mouse or human embryonic stem cell-derived cortical neurons have indicated that host brain can influence the activity of grafted neurons. Bragin *et al.* (1988) observed that a majority of neurons in implants of embryonic somatosensory cortex placed in the barrel field of adult rat responded with normal latency ranges to whisker displacement. Girman and Golovina (1990) found that the majority of neurons within transplants of rat embryonic occipital cortex placed in the primary visual cortex in adult rats responded to visual stimuli. Consistent with our observations using the rabies virus-based method, experiments with injection of a retrograde tracer in embryonic tissue transplants provided evidence that the host brain afferents to the grafts were the same as those innervating the intact visual cortex replaced by the grafts (Girman, 1994; Gaillard *et al.*, 1998). Recently, Michelsen *et al.* (2015) implanted cortically fated neurons, derived from mouse embryonic stem cells, into a neurotoxin-induced lesion in adult mouse visual cortex. Host neurons established synaptic contacts with grafted neurons and injection of an anterograde tracer into geniculate nucleus or contralateral visual cortex labelled fibres inside the graft. The mouse embryonic stem cell-derived grafted neurons responded to light stimulation.

In line with previous studies using embryonic mouse cortical cells (Fricker-Gates *et al.*, 2002; Gaillard *et al.*, 2007), Michelsen *et al.* (2015) have provided evidence indicating that the magnitude of efferents and afferents and level of functional integration after transplantation of mouse embryonic stem cell-derived neurons into adult mouse brain are mainly dependent on the degree of identity match between transplanted cells and injured cortex. We show here extensive connections including appropriate thalamic inputs and functional integration of grafted neurons in rats with

stroke-induced injury in somatosensory cortex. Our findings suggest that these xenografted human-derived cells, fated towards a cortical phenotype, provide a rather precise match to the areal identity of the lesioned neurons, i.e. somatosensory cortical neurons.

We have previously shown that intracortical implantation of lt-NES cell-derived cortical neurons in the dMCAO model leads to partial recovery of sensorimotor function (Tornero *et al.*, 2013). The present findings raise the possibility that the establishment of direct synaptic inputs to grafted neurons, e.g. from ventral and posterior thalamic nuclei and contralateral cortex, and their activation by physiological sensory stimuli contribute to the functional recovery at 8 weeks. At this time point, the majority of cells in the graft stained for immature and mature neuronal markers, and efferent projections were detected in ipsi- and contralateral cortex with a few reaching subcortically along the internal capsule (Tornero *et al.*, 2013). However, the main mechanism underlying the improvement at 8 weeks is probably not neuronal replacement but other mechanisms such as modulation of inflammation and trophic effects (Tornero *et al.*, 2013). Most likely, functional restoration due to integration of grafted neurons and reconstruction of circuitry develops slowly, reaching its maximum at later time points, and only plays a minor role at 8 weeks. When analysed at 5 months, grafted cells exhibited the electrophysiological properties of mature neurons (Tornero *et al.*, 2013). Illustrating the slow and protracted development of transplanted human neurons, Espuny-Camacho *et al.* (2013) observed that the level of innervation of the host brain from human embryonic stem cell-derived neurons implanted into neonatal mouse cortex increased markedly between 2 and 6 months. Similarly, when human non-fated lt-NES cell-derived neurons were implanted in rat hippocampus or on organotypic mouse hippocampal slice cultures, optogenetic stimulation of host neurons revealed more mature intrinsic properties of the grafted cells and extensive synaptic afferents at 6 months as compared to 6 weeks (Avaliani *et al.*, 2014).

The present findings should also be considered from a clinical perspective. The cortical neurons generated by reprogramming of adult human somatic cells receive direct afferent synaptic inputs from the appropriate areas of the stroke-injured brain, respond adequately to sensory stimulation, and send widespread projections to other brain areas (Tornero *et al.*, 2013). Thus, these neurons become morphologically and, at least some of them, also functionally incorporated into neural circuitries in the stroke-injured adult brain. It remains to be demonstrated, though, that this mechanism will lead to further amelioration of the functional impairments at longer time-points after the insult. Although only representing a first and early step in a clinical translation, our study illustrates the potential of functional restoration by cortical neuronal replacement as a future therapeutic approach for human neurodegenerative diseases affecting cerebral cortex.

Acknowledgements

We thank Dr Henrik Ahlenius for help with preparation of lentivirus and discussions, Bengt Mattsson for illustrations, Dr Johan Jakobsson for providing the virus for optogenetic control, Dr Tania Ramos for technical help with optogenetics set-up and Linda Jansson for technical assistance.

Funding

This work was supported by Swedish Research Council, European Union projects TargetBraIn (279017) and NeuroStemCellRepair (602278), Region Skåne, Sparbanksstiftelsen Färs & Frosta, Swedish Brain Foundation, Ragnar Söderberg Foundation, Stroke-Riksförbundet and Swedish Government Initiative for Strategic Research Areas (StemTherapy). C.R. was supported by a post-doctoral "Sara Borrel" grant from Spanish Government. S.G. was supported by a post-doctoral stipend from the Swedish Brain Foundation. M.P. is funded by ERC Grant Agreement n. 309712.

Supplementary material

Supplementary material is available at *Brain* online.

References

Aguilar J, Morales-Botello ML, Foffani G. Tactile responses of hindpaw, forepaw and whisker neurons in the thalamic ventrobasal complex of anesthetized rats. Eur J Neurosci. 2008; 27: 378–87.

Allison T, McCarthy G, Wood CC, Williamson PD, Spencer DD. Human cortical potentials evoked by stimulation of the median nerve. II. Cytoarchitectonic areas generating long-latency activity. J Neurophysiol 1989; 62: 711–22.

Avaliani N, Sorensen AT, Ledri M, Bengzon J, Koch P, Brustle O, et al. Optogenetics reveal delayed afferent synaptogenesis on grafted human-induced pluripotent stem cell-derived neural progenitors. Stem Cells 2014; 32: 3088–98.

Bragin AG, Bohne A, Vinogradova OS. Transplants of the embryonal rat somatosensory neocortex in the barrel field of the adult rat: responses of the grafted neurons to sensory stimulation. Neuroscience 1988; 25: 751–8.

Buhnemann C, Scholz A, Bernreuther C, Malik CY, Braun H, Schachner M, et al. Neuronal differentiation of transplanted embryonic stem cell-derived precursors in stroke lesions of adult rats. Brain 2006; 129 (Pt 12): 3238–48.

Buzsaki G. Large-scale recording of neuronal ensembles. Nat Neuroscience 2004; 7: 446–51.

Chapin JK, Sadeq M, Guise JL. Corticocortical connections within the primary somatosensory cortex of the rat. J Comp Neurol 1987; 263: 326–46.

Daadi MM, Lee SH, Arac A, Grueter BA, Bhatnagar R, Maag A-L, et al. Functional engraftment of the medial ganglionic eminence cells in experimental stroke model. Cell Transpl 2009; 18: 815–26.

Deshpande A, Bergami M, Ghanem A, Conzelmann KK, Lepier A, Gotz M, et al. Retrograde monosynaptic tracing reveals the temporal evolution of inputs onto new neurons in the adult dentate gyrus and olfactory bulb. Proc Natl Acad Sci U S A 2013; 110(12): E1152–61.

Dull T, Zufferey R, Kelly M, Mandel RJ, Nguyen M, Trono D, et al. A third-generation lentivirus vector with a conditional packaging system. J Virol 1998; 72(11): 8463–71.

Espuny-Camacho I, Michelsen Kimmo A, Gall D, Linaro D, Hasche A, Bonnefont J, et al. Pyramidal neurons derived from human pluripotent stem cells integrate efficiently into mouse brain circuits in vivo. Neuron 2013; 77: 440–56.

Etessami R, Conzelmann KK, Fadai-Ghotbi B, Natelson B, Tsiang H, Ceccaldi PE. Spread and pathogenic characteristics of a G-deficient rabies virus recombinant: an in vitro and in vivo study. J Gen Virol 2000; 81(Pt 9): 2147–53.

Fame RM, MacDonald JL, Macklis JD. Development, specification, and diversity of callosal projection neurons. Trends Neurosci 2011; 34: 41–50.

Fricker-Gates RA, Shin JJ, Tai CC, Catapano LA, Macklis JD. Late-stage immature neocortical neurons reconstruct interhemispheric connections and form synaptic contacts with increased efficiency in adult mouse cortex undergoing targeted neurodegeneration. J Neurosci 2002; 22: 4045–56.

Gaillard F, Girman SV, Gaillard A. Afferents to visually responsive grafts of embryonic occipital neocortex tissue implanted into V1 (Oc1) cortical area of adult rats. Restor Neurol Neurosci 1998; 12: 13–25.

Gaillard A, Prestoz L, Dumartin B, Cantereau A, Morel F, Roger M, et al. Reestablishment of damaged adult motor pathways by grafted embryonic cortical neurons. Nat Neurosci 2007; 10: 1294–9.

George PM, Steinberg GK. Novel stroke therapeutics: Unraveling stroke pathophysiology and its impact on clinical treatments. Neuron 2015; 87: 297–309.

Girman SV. Neocortical grafts receive functional afferents from the same neurons of the thalamus which have innervated the visual cortex replaced by the graft in adult rats. Neuroscience 1994; 60: 989–97.

Girman SV, Golovina IL. Electrophysiological properties of embryonic neocortex transplants replacing the primary visual cortex of adult rats. Brain Res 1990; 523: 78–86.

Grabowski M, Brundin P, Johansson BB. Functional integration of cortical grafts placed in brain infarcts of rats. Ann Neurol 1993; 34: 362–8.

Grealish S, Heuer A, Cardoso T, Kirkeby A, Jonsson M, Johansson J, et al. Monosynaptic tracing using modified rabies virus reveals early and extensive circuit integration of human embryonic stem cell-derived neurons. Stem Cell Rep 2015; 4: 975–83.

Harris KM, Kater SB. Dendritic spines: cellular specializations imparting both stability and flexibility to synaptic function. Ann Rev Neurosci 1994; 17: 341–71.

Hur EE, Zaborszky L. Vglut2 afferents to the medial prefrontal and primary somatosensory cortices: a combined retrograde tracing in situ hybridization study [corrected]. J Comp Neurol 2005; 483: 351–73.

Kalliomaki J, Weng HR, Nilsson HJ, Yu YB, Schouenborg J. Multiple spinal pathways mediate cutaneous nociceptive C fibre input to the primary somatosensory cortex (SI) in the rat. Brain Res 1993; 622: 271–9.

Kanno A, Nakasato N, Hatanaka K, Yoshimoto T. Ipsilateral area 3b responses to median nerve somatosensory stimulation. Neuroimage 2003; 18: 169–77.

Koch P, Opitz T, Steinbeck JA, Ladewig J, Brustle O. A rosette-type, self-renewing human ES cell-derived neural stem cell with potential for in vitro instruction and synaptic integration. Proc Natl Acad Sci U S A 2009; 106: 3225–30.

Kokaia Z, Martino G, Schwartz M, Lindvall O. Cross-talk between neural stem cells and immune cells: the key to better brain repair? Nat Neurosci 2012; 15: 1078–87.

Leisman G, Melillo R. The basal ganglia: motor and cognitive relationships in a clinical neurobehavioral context. Rev Neurosci 2013; 24: 9–25.

Lepore AC, Neuhuber B, Connors TM, Han SSW, Liu Y, Daniels MP, et al. Long-term fate of neural precursor cells following transplantation into developing and adult CNS. Neuroscience 2006; 142: 287–304.

Liang Z, Li T, King J, Zhang N. Mapping thalamocortical networks in rat brain using resting-state functional connectivity. Neuroimage 2013; 83: 237–44.

Lindvall O, Kokaia Z. Stem cell research in stroke: how far from the clinic? Stroke 2011; 42: 2369–75.

Michelsen KA, Acosta-Verdugo S, Benoit-Marand M, Espuny-Camacho I, Gaspard N, Saha B, et al. Area-specific reestablishment of damaged circuits in the adult cerebral cortex by cortical neurons derived from mouse embryonic stem cells. Neuron 2015; 85: 982–97.

Moxon KA, Hale LL, Aguilar J, Foffani G. Responses of infragranular neurons in the rat primary somatosensory cortex to forepaw and hindpaw tactile stimuli. Neuroscience 2008; 156: 1083–92.

Muneton-Gomez VC, Doncel-Perez E, Fernandez AP, Serrano J, Pozo-Rodrigalvarez A, Vellosillo-Huerta L, et al. Neural differentiation of transplanted neural stem cells in a rat model of striatal lacunar infarction: light and electron microscopic observations. Front Cell Neurosci 2012; 6: 30.

Oki K, Tatarishvili J, Wood J, Koch P, Wattananit S, Mine Y, et al. Human-induced pluripotent stem cells form functional neurons and improve recovery after grafting in stroke-damaged brain. Stem Cells 2012; 30: 1120–33.

Osakada F, Callaway EM. Design and generation of recombinant rabies virus vectors. Nat Protoc 2013; 8: 1583–601.

Paxinos G, Watson C. The rat brain in stereotaxic coordinates. 4th ed. ed. San Diego: Academic Press; 1998.

Schneggenburger R, Sakaba T, Neher E. Vesicle pools and short-term synaptic depression: lessons from a large synapse. Trends Neurosci 2002; 25: 206–12.

Thorbergsson PT, Garwicz M, Schouenborg J, Johansson AJ. Spike-feature based estimation of electrode position in extracellular neural recordings. Conf Proc IEEE Eng Med Biol Soc 2012; 2012: 3380–3.

Tornero D, Wattananit S, Gronning Madsen M, Koch P, Wood J, Tatarishvili J, et al. Human induced pluripotent stem cell-derived cortical neurons integrate in stroke-injured cortex and improve functional recovery. Brain 2013; 136(Pt 12): 3561–77.

Tsupykov O, Kyryk V, Smozhanik E, Rybachuk O, Butenko G, Pivneva T, et al. Long-term fate of grafted hippocampal neural progenitor cells following ischemic injury. J Neurosci Res 2014; 92: 964–74.

Tutunculer B, Foffani G, Himes BT, Moxon KA. Structure of the excitatory receptive fields of infragranular forelimb neurons in the rat primary somatosensory cortex responding to touch. Cereb Cortex 2006; 16: 791–810.

Vivar C, Potter MC, Choi J, Lee JY, Stringer TP, Callaway EM, et al. Monosynaptic inputs to new neurons in the dentate gyrus. Nat Commun 2012; 3: 1107.

Wickersham IR, Lyon DC, Barnard RJ, Mori T, Finke S, Conzelmann KK, et al. Monosynaptic restriction of transsynaptic tracing from single, genetically targeted neurons. Neuron 2007; 53: 639–47.

Yamawaki N, Suter BA, Wickersham IR, Shepherd GM. Combining optogenetics and electrophysiology to analyze projection neuron circuits. Cold Spring Harb Protoc 2016; 2016: pdb prot090084.

Zakiewicz IM, Bjaalie JG, Leergaard TB. Brain-wide map of efferent projections from rat barrel cortex. Front Neuroinform 2014; 8: 5.